Cellular Signalling 58 (2019) 20–33

Contents lists available at ScienceDirect

Cellular Signalling

journal homepage: www.elsevier.com/locate/cellsig

Regulation of endothelial cell survival and death by the MAP kinase/ERK kinase kinase 3 - glyceraldehyde-3-phosphate dehydrogenase signaling axis

Yong Q. Li[a,b], Andy Ngo[a,b], Peter Hoffmann[c,d], Antonio Ferrante[a,b], Charles S. Hii[a,b,*]

[a] Department of Immunopathology, SA Pathology, Women's and Children's Hospital, North Adelaide, South Australia 5006, Australia
[b] Discipline of Paediatrics and the Robinson Research Institute, University of Adelaide, South Australia 5001, Australia
[c] Future Industries Institute, University of South Australia, Adelaide 5001, Australia
[d] Adelaide Proteomics Centre, University of Adelaide, 5001 Adelaide, South Australia 5006, Australia

ARTICLE INFO

Keywords:
Endothelial cell survival
Mitogen activated protein kinases
MAP kinase/ERK kinase kinase 3
Glyceraldehyde-3-phosphate dehydrogenase
Protein-protein interaction

ABSTRACT

Endothelial cell injury and death precede atherosclerosis development. Thus, it is important to understand the mechanisms that lead to these early changes in endothelial cells. Although members of the MAP kinase/ERK kinase (MEK) kinase 3 (MEKK3)-MEK5-ERK5 module play an essential role in underpinning endothelial cell survival, how they execute these actions remain poorly understood. Furthermore, there is poor understanding of death-inducing pathways in endothelial cells and it is also unclear whether there are direct interactions between the kinase module and death-inducing pathways. Using immunoprecipitation and liquid chromatography-electrospray ionisation tandem mass spectrometry approaches, we show in human umbilical vein endothelial cells that the MEKK3-MEK5-ERK5 ternary complex contains glyceraldehyde-3-phosphate dehydrogenase (GAPDH), a glycolytic enzyme that can trigger the death of certain cell-types. GAPDH binds directly to MEKK3. Interestingly, serum depletion, a trigger of endothelial cell death, results in a rapid loss of cytosolic MEKK3 and MEKK3-GAPDH interaction. MEKK3 rapidly reappears in the cytosol upon serum replenishment, accompanied by the restoration of MEKK3-GAPDH interaction. During serum starvation or exposure to cytotoxic concentrations of H_2O_2, GAPDH accumulates in the nucleus. Inhibition of the nuclear accumulation of GAPDH with R-(−)-deprenyl hydrochloride attenuates the degree of cell death. Serum replenishment of serum-starved cells reduces the level of nuclear GAPDH and prevents cell death. Cell-free assays show phosphorylation of GAPDH on four residues by MEKK3. These data not only strongly implicate nuclear GAPDH in causing endothelial cell death but also reveal a potential mechanism for MEKK3 to regulate GAPDH function and hence promote endothelial cell survival.

1. Introduction

Atherosclerosis is a chronic inflammatory condition that underlies the majority of coronary artery-related events and stroke. Risk factors for this disease include hypertension, obesity, diabetes mellitus, dyslipidaemia, advancing age, tobacco smoking, inflammatory conditions and genetic predisposition [1]. A common link between the modifiable factors is chronic oxidative stress in the blood vessels through increased production of reactive oxygen species such as the superoxide anion. This leads to altered levels of nitric oxide and to the formation of hydrogen peroxide (H_2O_2) through superoxide dismutation. Although low levels of H_2O_2 contribute to homeostasis, high levels can directly cause endothelial cell injury or death by apoptosis [2], a major factor that contributes to endothelial dysfunction [3]. A consequence of this dysfunctional state is the retention of apolipoprotein B-containing lipoproteins in the subendothelial space of lesion-prone areas of the arterial tree [1,3,4], thereby underpinning atherogenesis. Thus, preventing the injury or death of these cells is likely to attenuate or impede atherogenesis.

Serum plays an essential role in maintaining the survival of endothelial cells [5]. Its absence results in the accumulation of reactive oxygen species in endothelial cells [6], making serum-deprivation a popular in vitro model to investigate the basis of endothelial dysfunction. One of the signaling pathways that mediates the survival-

Abbreviations: MAP kinase, Mitogen-Activated Protein kinase; ERK kinase, Extracellular signal-Regulated protein Kinase; MEK, MAP kinase/ERK Kinase; MEKK, MEK Kinase; HUVEC, human umbilical vein endothelial cells

* Corresponding author at: Department of Immunopathology, SA Pathology at the Women's and Children's Hospital, 72 King William Road, North Adelaide, South Australia 5006, Australia.

E-mail addresses: Peter.Hoffmann@unisa.edu.au (P. Hoffmann), antonio.ferrante@adelaide.edu.au (A. Ferrante), charles.hii@adelaide.edu.au (C.S. Hii).

https://doi.org/10.1016/j.cellsig.2019.03.002
Received 15 January 2019; Received in revised form 1 March 2019; Accepted 1 March 2019
Available online 02 March 2019
0898-6568/

promoting function of serum is the MEKK3-ERK5 module [5] that exists in cells as a three kinase complex consisting of a MAP kinase kinase kinase (MEKK2 or MEKK3), a MAP kinase kinase (MEK5) and a MAP kinase (ERK5) [7]. With the exception of MEKK2, all kinases in the ERK5 module are vital for the development of the cardiovascular system. Deletion of MEKK3, MEK5 or ERK5 results in embryonic death at ≈E10.5, due to angiogenic failure, cardiac defects and associated endothelial cell apoptosis [8–11]. Furthermore, conditional deletion of ERK5 in adult mice resulted in endothelial cell death and a fatal phenotype [12]. Despite their importance, the mechanisms via which these kinases act remain poorly understood. Similarly, the basis for the death of endothelial cells in the kinase-null mice remains unclear but could involve the activation of a death mechanism in the absence of the kinases.

The aims of this study were to investigate the mechanism via which the MEKK3-ERK5 module maintains endothelial cell survival, identify novel triggers of endothelial cell death and to determine whether there is cross-talking between the kinase module and death-inducing pathways. Our data not only show that an increase in nuclear GAPDH promotes endothelial cell death but also suggest a new mechanism via which MEKK3 is able to directly regulate GAPDH function and hence promote endothelial cell survival.

2. Materials and methods

2.1. Materials

RPMI-1640, FCS, Hanks' balanced salt solution (HBSS), R-(−)-deprenyl.HCl, gelatin and the Duolink Proximity Ligation Assay reagents (DUO92001, DUO92005, DUO92014, DUO82049 and DUO82040) for mouse/rabbit combination and for green detection were obtained from Sigma-Aldrich (Castle Hill, NWS, Australia). Ficoll-Paque Plus was purchased from GE Healthcare Bio-Sciences AB (Uppsala, Sweden). *E*-Coli-expressed GST-MEK5 and GST-MEKK3 were obtained from Abnova Corp. (Taipei, Taiwan) while active GST-MEKK3, expressed by baculovirus in Sf9 insect cells, was purchased from SignalChem (Richmond, BC, Canada). Type 2 collagenase (from *Clostridium histolyticum*) was purchased from Worthington Biochem. Corp (Lakewood, NJ). Human recombinant GAPDH was obtained from Prospec-Tany TechnoGene Ltd. Ness-Ziona, Israel). γ-^{32}P-ATP (4000 Ci/mmol) was obtained from PerkinElmer (Melbourne, Vic, Australia). Reinforced nitrocellulose was purchased from Thermo Fisher Scientific (Scoresby, Vic, Australia). Western blot recycling kits were obtained from Alpha Diagnostic International (San Antonio, Tx).

2.2. Antibodies

Rabbit polyclonal anti-ERK5 (E1523) and mouse monoclonal anti-GAPDH (G8795) antibodies were purchased from Sigma-Aldrich (Castle Hill, NSW, Australia). Rabbit polyclonal anti-GAPDH antibody (OAAB19507) was obtained from Aviva Systems Biology (San Diego, CA). Mouse monoclonal anti-GAPDH (0411) antibody (sc-47,724), rabbit polyclonal anti-lactate dehydrogenase (LDH) antibody (sc-33,781), goat anti-histone H2B antibody (sc-8650), rabbit polyclonal anti-ERK2 antibody (sc-154) and mouse IgG_1 isotype (sc-3877) were purchased from Santa Cruz Biotechnology (Dallas, Tx). Rabbit polyclonal anti-MEKK3 (N3C3) antibody (GTX107945) was obtained from GeneTex Inc. (Irvine, CA). Rabbit polyclonal anti-MEK5 antibody (ADI-KAP-MA003-E) and mouse monoclonal anti-MEK5 antibody (MA5–19711) were purchased from Stressgen Biotechnologies/Enzo Life Sciences (Farmingdale, NY) and ThermoFisher (Scoresby, Vic. Australia), respectively. All secondary antibodies were from Dako (Agilent Technologies, Mulgrave, Vic, Australia). OKT3 anti-CD3 antibody was obtained from Abcam (Melbourne, Vic, Australia)((Cat#ab86883) and functional grade anti-CD28 antibody (clone CD28.2, Cat 16–0289-81) was from ThermoFisher (Scoresby, Vic. Australia).

2.3. Preparation of human group AB serum

To prepare serum for cell culture, blood was obtained with informed consent from several adult donors with AB blood type, approved by our institution's Human Ethics Committee. The collected blood was allowed to clot overnight. The serum was then collected, pooled and aliquoted before being stored in a -20° C freezer. The collection of blood was approved by our institution's Human Ethics Committee.

2.4. Preparation and culture of HUVEC

Human umbilical vein endothelial cells (HUVEC) were isolated from umbilical cords by collagenase digestion of the interior of the umbilical vein as described previously [13] with minor modifications. Collection of the cords was approved by our institution's Human Ethics Committee. Briefly, for each cord, the vein was cannulated, filled with warm type 2 collagenase (0.4 mg/ml, 215 U/mg) in HBSS and incubated with massaging for ~2 min at 37 °C. After flushing the digest out of the vein, the cells were centrifuged (400*g* × 10 min), resuspended in RPMI-1640 containing penicillin (80 U/ml), streptomycin (80 μg/ml), 3.2 mM L-glutamine, and 20% (*v*/v) pooled heat-inactivated (56° C, 30 min) human group AB serum and distributed to gelatin-precoated (0.1%, *w*/*v*) tissue culture flasks (75 cm^2, Corning). The cultures were grown at 37 °C in a humidified atmosphere of 5% CO_2 in air. On the fourth day, the confluent flasks were washed and the cells plated on gelatin (0.2% w/v)-coated plates. Endothelial cells were identified by their characteristic monolayer cobblestone appearance and positive staining for von Willebrand factor as described previously [14].

2.5. Preparation and culture of human peripheral blood T cells

Human blood was obtained by venipuncture from healthy donors in the Women's and Children's Hospital, with approval from our institution's Human Ethics Committee. T cells were prepared from the mononuclear cell fraction as described [15]. Briefly, to obtain mononuclear cells, the blood was layered on Ficoll Hypaque (density of 1.114 *g*/ml). Following centrifugation, the resultant leukocyte fraction was applied to Ficoll-Paque Plus, centrifuged and the cells were incubated in plastic tissue culture dishes. The non-adherent lymphocyte fraction was collected and passed through two cycles of nylon wool columns. The T cells that were eluted were at least 95% pure and 99% viable. The cells were then cultured in RPMI-1640 in the presence of human Ab serum (5%) and used within 24 h after preparation.

2.6. Incubations and cell viability assays

To isolate proteins that interact with the MEKK3-ERK5 complex, cells were incubated in the presence or absence of various agents, harvested at various times and lysed. Cell viability was determined by the trypan blue exclusion test.

2.7. Preparation of cell lysates

Endothelial cell lysates were prepared as described previously [16]. Briefly, the cells were lysed in 300 μl of cold lysis buffer A (20 mM HEPES, pH 7.4, 0.5% NP40 (*v*/v), 100 mM NaCl, 1 mM EDTA, 2 mM Na_3VO_4, 2 mM DTT, 1 mM PMSF, 2 mM *p*-nitrophenylphosphate and 10 μg/ml each of leupeptin, aprotinin, pepstatin A and benzamidine) for 2 h (4° C) with constant mixing. Cell debris was sedimented (12,000 g × 30 s) and the protein content of the soluble fractions was determined by the Lowry's protein estimation method.

2.8. Preparation of nuclear and cytosolic fractions

Nuclear fractions were prepared by the rapid technique described by Andrews and Faller [17] with some modifications. Briefly, washed

cells were scrapped in 200 µl of cold lysis buffer B (10 mM HEPES-KOH, pH 7.9, 1.5 mM $MgCl_2$, 10 mM KCl, 0.5 mM dithiothreitol and the above protease inhibitors) and allowed to swell for 30 min with rotation (4° C). Following vigorous vortexing (45 s at 4° C), the cells were centrifuged (12,000*g* × 2 min). The supernatants were kept as cytoplasmic fractions. The pellets were washed 2× with buffer B and then resuspended in cold buffer C (20 mM HEPES-KOH, pH 7.9, 25% glycerol, 420 mM NaCl, 1.5 mM $MgCl_2$, 0.2 mM EDTA, 0.5 mM DTT and protease inhibitors) and incubated for 20 min with rotation (4 °C), followed by centrifugation (12,000*g* × 2 min). The supernatants were collected. The protein content of the supernatants was determined and the samples stored at -20° C. Histone H2B and lactate dehydrogenase (LDH), detected by western blotting, were used as markers of nuclear and cytosolic fractions, respectively.

2.9. Immunoprecipitation, GST-glutathione pull-down and phosphorylation assays

For immunoprecipitation, cell lysates were precleared to remove non-specifically bound proteins. The precleared samples (around 0.5–0.8 mg total protein) were then incubated with an antibody or IgG (3 µg each) against the target for 2 h at 4° C with constant mixing. The kinases/proteins were precipitated with fresh protein A sepharose and washed 3× with buffer A as described previously [16]. These were used for mass spectrometry after SDS PAGE, phosphorylation assays or western blotting. For pull-down assays, recombinant proteins were incubated as described in figure legends and precipitated by adding glutathione sepharose (20 µl of a 1:1 slurry). For phosphorylation assays, the precipitates were washed once with buffer A and once with assay buffer at 4 °C [16]. To examine the phosphorylation of recombinant GAPDH by recombinant MERKK3, the two proteins were premixed before the assay. The assay was started by adding 30 µl of assay buffer (30 °C) containing either 10 µCi of [γ-32P]ATP or unlabelled ATP and 3.8 mM *p*-nitrophenyl phosphate. After 20 or 40 min, Laemmli buffer was added and the samples boiled for 5 min at 100 °C. Phosphorylated proteins were fractionated by SDS PAGE and radiolabelled proteins were detected and quantitated using an Instant Imager (Packard Instruments) whereas the non-radiolabelled proteins were used in downstream mass spectrometry.

2.10. Proximity ligation assay

HUVEC, in complete medium (40 µl), were placed on gelatin-coated microscope cover glass and incubated overnight in a humidified atmosphere of 5% CO_2 in air. The cells were then treated as follows: unwashed, washed and incubated in serum-free medium (30 min), or washed, incubated in serum-free medium followed by incubation (30 min) in serum-replete medium. The cells were fixed in 4% paraformaldehyde–PBS and permealised with 0.2% NP-40 (10 min incubation at room temperature). Human T cells were either unstimulated or stimulated with plate-bound anti-CD3 antibody (1 µg/ml) and soluble anti-CD28 antibody (0.5 µg/ml) for 1 h, after which they were cyto-centrifuged onto glass slides, fixed and permeabilised as described above. The proximity ligation assay was conducted according to the manufacturer's instructions. The antibodies used were mouse anti-GAPDH antibody (0411) (sc-47,724, Santa Cruz Biotechnology, Dallas, Tx) (1:100 dilution) and rabbit anti-MEKK3 antibody (GTX107945, GeneTex Inc., Irvine, CA) (1:100 dilution). As a negative control, a mouse IgG_1 isotype (1:100 dilution) was added with anti-MEKK3 antibody. The pieces of cover glass were mounted on microscope slides and images viewed (1000×, oil immersion) under an Olympus BX51 Fluorescence Microscope (Olympus Australia, Notting Hill, Vic, Australia). Acquired images were superimposed using Adobe Photoshop CDS6 (Adobe Australia, Melbourne, Vic, Australia).

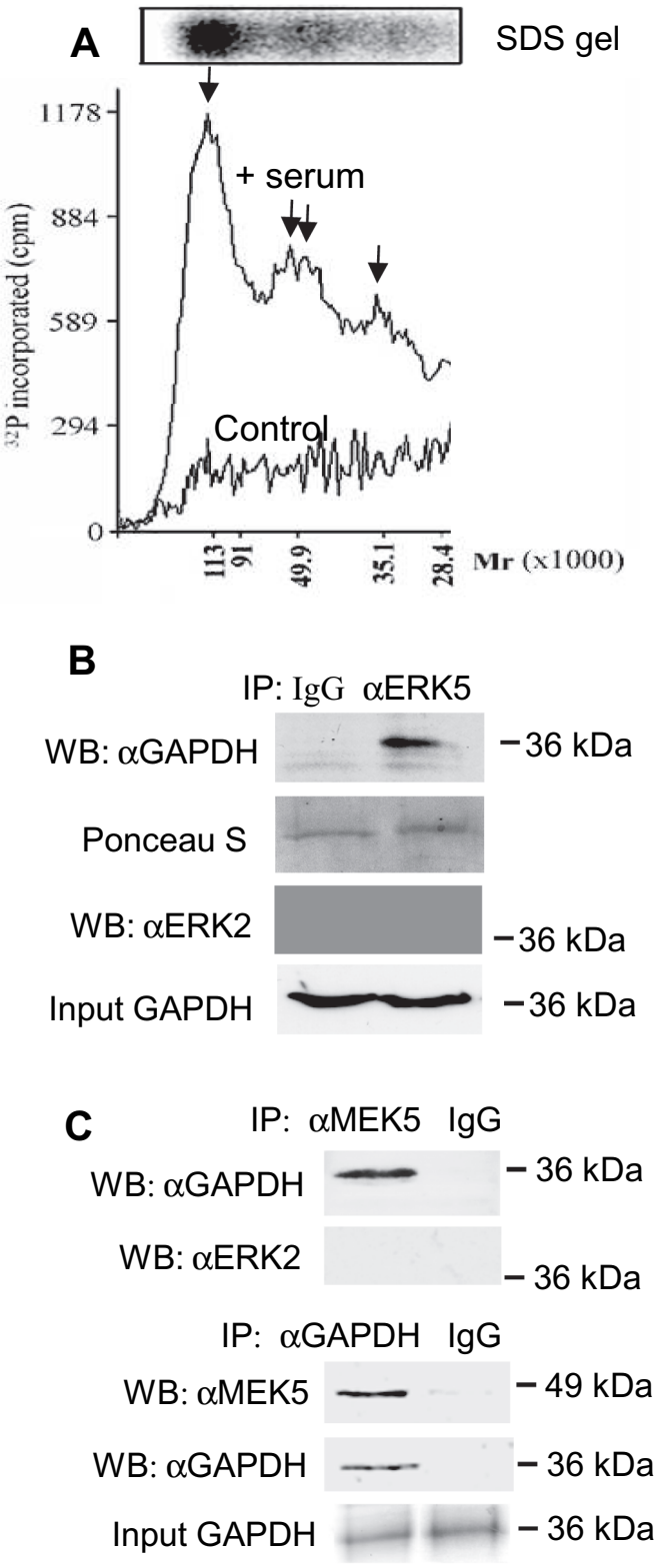

Fig. 1. Co-immunoprecipitation of GAPDH with members of the MEKK3-ERK5 module. (A) HUVEC were incubated in the presence or absence of serum, lysed and ERK5 was immunoprecipitated and incubated in kinase assay buffer containing [γ-^{32}P]ATP. Following fractionation by SDS PAGE (12% gel), phosphorylated proteins were detected in an Instant Imager. A representative radiogram and radioactivity profile of one of the gels are shown. Arrows indicate the positions of radioactive peaks. (B) Co-immunoprecipitation of GAPDH with ERK5. (C) Co-immunoprecipitation of GAPDH with MEK5. Results are representative of a minimum of three experiments using cells from different umbilical cords.

2.11. Western blot analysis

Lysate or nuclear proteins were fractionated by SDS PAGE and transferred to nitrocellulose. Prior to antibody staining, all membranes were stained with Ponceau S to determine the evenness in loading and transfer. If loading or transfer was found to be uneven, the SDS-PAGE and transfer steps were repeated. The amount of starting material or input protein of interest in each immunoprecipitation or assay was also determined by western blotting. All Santa Cruz antibodies were used at a dilution of 1:1000. The titres of the secondary antibodies for these blots were 1:1000 or 1:2000. The anti-ERK5 antibody was used at 1:500 and the secondary antibody was used at 1:2000. The rabbit polyclonal anti-MEK5 antibody was used at a titre of 1:500 and the secondary antibody was used at 1:1000. The anti-MEKK3 antibody and the secondary antibody were used at 1:2000. The mouse monoclonal anti-GAPDH antibody and the secondary antibodies were used at 1:10,000. Immunocomplexes were detected by enhanced chemiluminescence (ECL) [16] using the Biorad ChemiDoc XRS system. Band density was determined with the supplied software or Image Quant Software (GE Healthcare Life Science). Where appropriate, blots were stripped and reprobed with another antibody to confirm even loading or that similar amounts of a target protein had been immunoprecipitated, to assess the specificity of protein-protein interaction or to ascertain the purity of the cellular fractions.

2.12. Mass spectrometric analysis

2.12.1. Identification of co-immunoprecipitated proteins

Identification of co-immunoprecipitated proteins was performed as described below. SDS gels were stained with coomassie blue. Bands of interest were excised from the gel, destained and digested with 100 ng of trypsin per sample. Tryptic peptides were extracted and transferred in autosampler vial, vacuum concentrated and redissolved in 5 µl 1% formic acid in water. Then 5 µl tryptic peptides from each sample were chromatographed using an Agilent Protein ID Chip column assembly (40 nl trap column with 0·075 × 43 mm C-18 analytical column) housed in an Agilent HPLC-Chip Cube Interface connected to an a HCT ultra 3D-Ion-Trap mass spectrometer (Bruker Daltonik GmbH). The column was equilibrated with 4% acetonitrile (ACN) / 0·1% FA at 0·5 µl/min and the samples eluted with an ACN gradient (4%–30% in 30 min). Ionisable species ($300 < m/z < 1200$) were trapped and one or two of the most intense ions eluting at the time were fragmented by collision-induced dissociation. MS and MS/MS spectra were subjected to peak detection using DataAnalysis (Version 3.4, Bruker Daltonik GmbH). The combined MS and MS/MS mass lists were exported in Mascot generic format and submitted to the in-house Mascot database-searching engine (Matrix Science: http://www.matrixscience.com) using the following specifications: Taxonomy: *Mammalia* or *Homo sapiens;* Database: Swissprot 20,070,220; Enzyme: Trypsin; Fixed modifications: Carbamidomethyl (C); Variable modifications: Oxidation (M); Mass tol MS: 0.3 Da; MS/MS tol: 0.4 Da; Peptide charge: 1+, 2+ and 3+; Missed cleavages: 1. From a search against all mammalian proteins, the only significant matches to non-human proteins were to rabbit immunoglobulin or porcine trypsin. The search was then repeated against only human proteins. Identification of proteins within each band were based on a threshold score of 28, the number of queries matched or at least 2 unique matching queries if not the top hit, percentages of sequence coverage based on the MS/MS spectra and the observed and predicted molecular weights of the protein bands.

2.12.2. Identification of MEKK3 phosphorylation sites in GAPDH

Commasie blue-stained GAPDH band was excised from the gels, destained and subjected to trypsin or Asp-N digestion. The volume of the extracted peptides was reduced by vacuum centrifugation and then resuspended with 0.1% FA in 2% CAN. Peptides were separated on a HPLC system (Thermo Scientific) using a separation column (Thermo Scientific) (Acclaim PepMap RSLC, C18, pore size 100 Å, particle size 2 mm, 75 mm inner diameter (ID) × 15 cm length) and a trapping column (Thermo Scientific) (Acclaim PepMap100, C18, pore size 100 Å, particle size 3 mm, 75 mm ID × 2 cm length). The HPLC system was coupled to a LTQ Orbitrap XL mass spectrometer (Thermo Scientific), using the following buffer system: (A) 2% ACN, 0.1% FA in water; (B) 80% ACN, 0.1% FA in water. For in-line desalting and concentration, 1 ml of digests were loaded onto the trap column and the washed for 5 min with 100% A at a flow rate 5 ml/min. Peptides were eluted at 300 nl/min flow rate with the following 55 min gradient: 4% B for 10 min, gradient to 40% B over 20 min, gradient to 90% B in 30 s, 90% B for 9.5 min, gradient from 90% to 4% B in 30 s, 4% B for 15.5 min. Full scan mass spectra were acquired in the Orbitrap over m/z 300–2000. The six most intense multiply charged ions above an intensity threshold of 1000 were selected for collision-induced dissociation (CID) in the linear ion trap at normalized collision energy of 35%. If an ion was selected for CID, dynamic exclusion was used to exclude it, and all other ions within ± 10 ppm, from repeated CID measurement for a period of 48 s. The GAPDH sample was run a second time with the same settings as above with the following modifications: dynamic exclusion of repeat CID of ions within -0.8 to $1.5\ m/z$ for a period of 15 s and where an ion resulting from a neutral loss corresponding to phosphorylation was observed as one of the 3 most abundant fragment ions, it was subjected to a second CID event. Raw data files were subjected to the Proteome Discoverer software (Thermo Scientific) to set up the workflow, files were then submitted to MASCOT (Version 2.2; Matrix Science Inc.: Boston, USA, 2007) by the Proteome Discoverer Daemon (Thermo Scientific). Peak lists in the range from 350 m/z to 5000 m/z were searched against the SwissProt 2013_04 database.

Table 1
Proteins that co-immunoprecipitated with ERK5.

Function	Proteins
Energy metabolism	
Glycolysis	G3P, LDHA, LDHB, PGK1, PKM/KPYM
Oxidative phosphorylation	ATPO, ETFA, UQCR2, PHB2
Mitochondrial function	HSP60, VDAC-1, ADT2
Proliferation/survival/death	PHB2, HSP60, VDAC1, CLIC1, CLIC4
Protein synthesis	IF4A1, rpS2, rpS3, rpS4X, rpS19, rpL23A, rpL24, rpS4X, rpL7, rpL7A, rpS6, GBLP, VIME
Protein folding/Chaperones	TCP-1-alpha, TCP-1-eta, PPIB
Others	ACTB, ACTG

G3P: Glyceraldehyde-3-phosphate dehydrogenase; LDHA or B: L-lactate dehydrogenase A or B chain; PGK1: Phosphoglycerate kinase 1; PKM/KPYM: Pyruvate kinase isozymes M1/M2; ATPO: ATP synthase O subunit, mitochondrial precursor; ETFA: Electron transfer flavoprotein subunit alpha, mitochondrial precursor; UQCR2: Ubiquinol-cytochrome-c reductase complex core protein 2, mitochondrial precursor; PHB2: Prohibitin-2; HSP60: 60 kDa heat shock protein; VDAC1: Voltage-dependent anion-selective channel protein 1; ADT2: ADP/ATP translocase 2; CLIC1 or 4: Chloride intracellular channel protein 1 or 4; IF4A1: Eukaryotic initiation factor 4A-I; rp: ribosomal protein; GBLP: Guanine nucleotide-binding protein subunit beta 2-like 1; VIME: Vimentin; TCP-1: T-complex protein 1; PPIB: Peptidyl-prolyl cis-trans isomerise B precursor.

2.13. Statistical analysis

Statistical analyses were performed using GraphPad InStat. Differences were analysed using Student's *t*-test, or Dunnett's or Bonferroni multiple comparisons test as appropriate and were considered significant when $P < 0.05$.

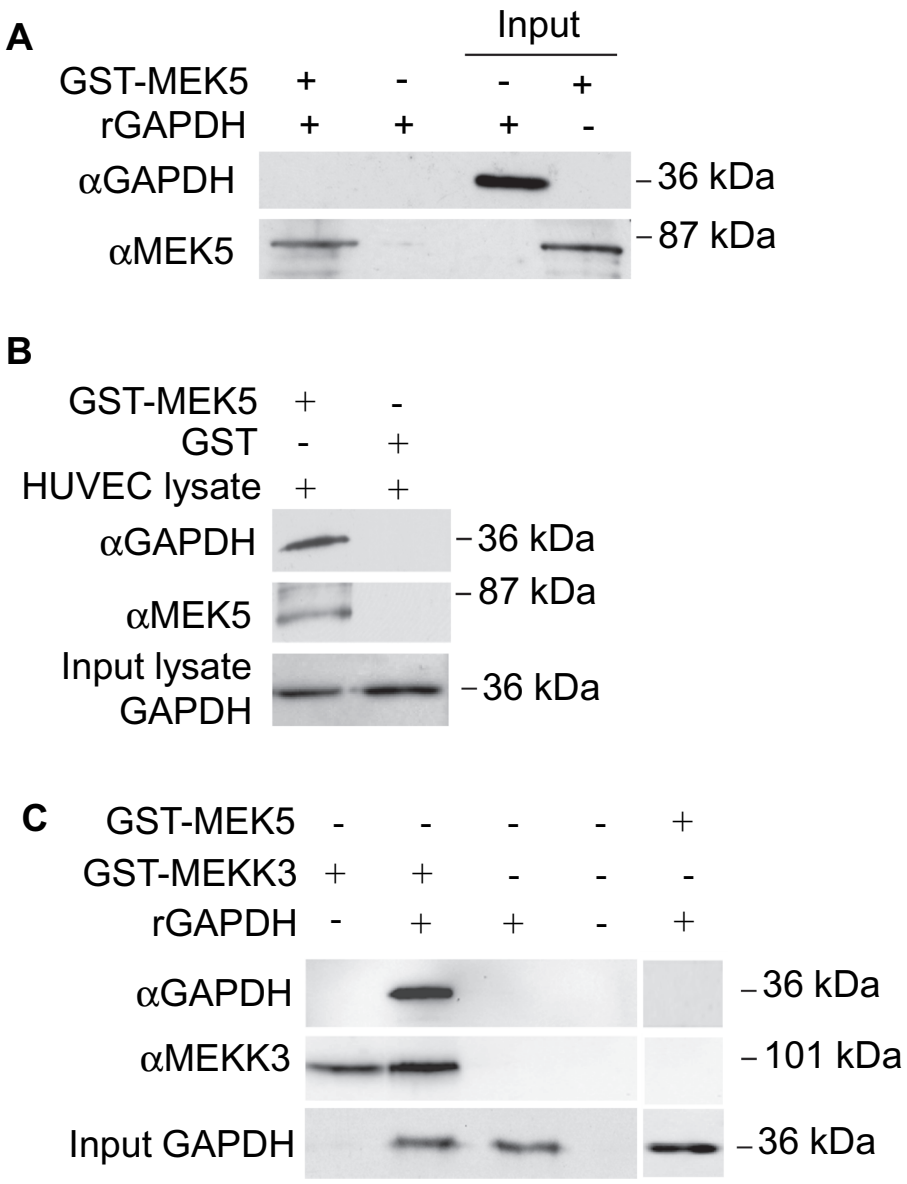

Fig. 2. Direct binding of GAPDH to MEKK3 but not to MEK5. (A) GST-MEK5 (0.1 μg) was incubated with recombinant GAPDH (0.1 μg). Following the addition of glutathione sepharose, the amount of bead-bound recombinant GAPDH was determined by western blotting with anti-GAPDH antibody. (B) GST-MEK5 was incubated with lysates of HUVEC (3 mg protein) and after precipitation with glutathione sepharose, pull-down of GAPDH was determined. Interaction between endothelial cell GAPDH and GST-MEK5 was detected. (C) GST-MEKK3 or GST-MEK5 (0.1 μg each) was incubated with recombinant GAPDH (0.1 μg). Following the addition of glutathione sepharose, the washed samples were western blotted with anti-GAPDH antibody. The data show binding of MEKK3 to GAPDH. The results are representative of 2 (A) – 3 (B and C) separate determinations.

3. Results

3.1. GAPDH binds to the MEKK3-MEK5-ERK5 ternary complex

To better understand the manner in which the MEKK3-ERK5 module protects endothelial cells, we reasoned that it would be important to identify the proteins that interact with the kinases or those that act as substrates, in order to guide investigations into the mechanism of action of the kinases. Because MEKK3(MEKK2), MEK5 and ERK5 exist in cells as a ternary complex in which MEK5 binds the upstream MEKK3(MEKK2) and downstream ERK5 via the Phox/Bem1p (PB1) domain of MEK5 [18,19], we immunoprecipitated ERK5 from the lysates of HUVEC that had been either serum-starved or incubated with fresh serum for 1 h. The samples were subjected to phosphorylation assays. Upon fractionation by SDS PAGE, radioactivity scanning of the gels revealed the presence of several peaks in samples from serum-stimulated cells (Fig. 1A). A major radioactive peak was found to migrate with an Mr. of ~113,000, the reported electrophoretic mobility of ERK5 in endothelial cells, consistent with serum causing ERK5 activation [20]. The peaks at an Mr. of ~50,000 were likely to contain MEK5 isoforms [21] that are substrates for ERK5 [22] and MEKK2/3 [7]. Another radioactive peak, although minor, was detected at M_r of ~36,000, thus signifying a potential substrate of the kinase module. To identify this and other interacting proteins, ERK5 from serum-stimulated HUVEC was immunoprecipitated and the sample subjected to SDS PAGE. The gels were stained with coomassie blue and the more densely-stained bands with Mr. ranging from 21,500 to 66,000 were excised. After tryptic digestion, the samples were subjected to Liquid chromatography-ESI mass spectrometry (MS & MS/MS).

The identified proteins could be grouped according to their function, determined by querying the gene ontology (GO) terms for biological processes (GO-Biological process). These processes include glucose metabolism, protein synthesis, protein folding and chaperones, and proliferation/cell death/differentiation (Table 1). Amongst the proteins with molecular weights of around 36 kDa were two glycolytic enzymes that are also known to regulate cell survival and death: lactate dehydrogenase, an inhibitor of apoptosis [23], and glyceraldehyde 3-phosphate dehydrogenase (GAPDH), a trigger of apoptosis in some cell-types when localised in the nucleus [24,25]. Because GAPDH is known to be phosphorylated in HeLa cells cultured the presence of serum [26] and serum regulates its subcellular localisation [27], we focussed our investigations on GAPDH. Immunoprecipitation with anti-ERK5 antibody and western

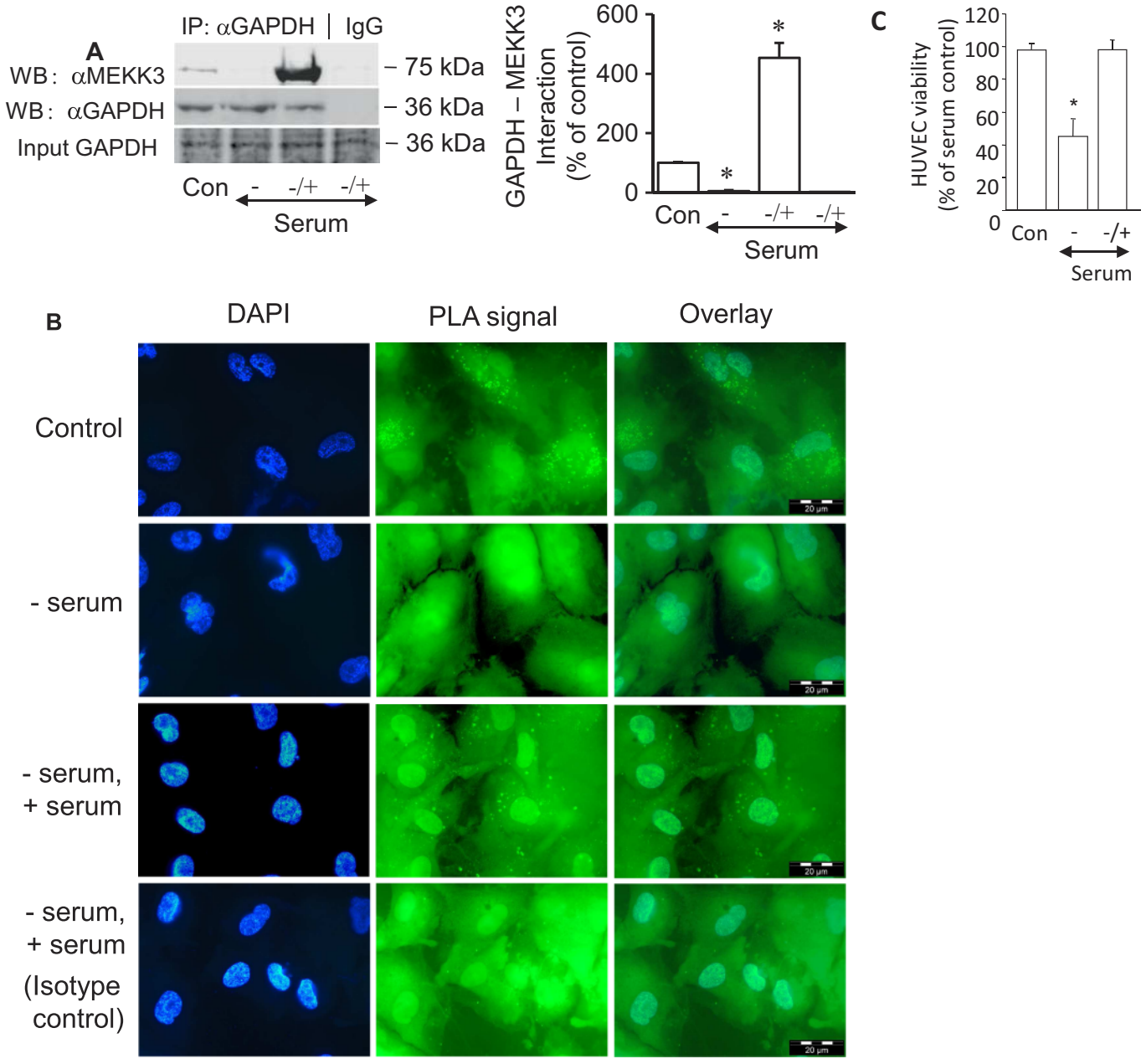

Fig. 3. GAPDH binds to MEKK3 in HUVEC. (A) Four sets of HUVEC were cultured for 4 days in the presence of 20% serum. One set of cells was lysed (Con) and the remaining sets were washed with serum-free medium and incubated in this medium for 1 h. Following this, one set was lysed (−) and serum (20%) was added to the remaining sets (±). After 30 min incubation, the cells were lysed and GAPDH-MEKK3 binding was determined. A representative blot and quantitated data (histogram, corrected for loading) (mean ± SEM, $n = 4$ experiments, each using a different batch of cells) are shown. Significance of difference from control: $^*p < 0.001$ (Dunnett's test). (B) Four sets of cells on microscope cover glass (in triplicate) were washed and incubated as described in (A). Following incubation, the cells were fixed and processed to determine GAPDH-MEKK3 binding by the PLA assay as described in Materials and Methods. The fluorescent dots represent GAPDH-MEKK3 interaction. Scale bar: 20 μm. Results shown are from a representative experiment ($n = 3$, all with similar results). (C) Effect of serum depletion and replenishment on HUVEC viability. Cells were washed and incubated in the absence of serum (−) or had the serum replenished after 1 h in serum-free medium (±). The viability of the cells was assessed 15 h later by the trypan blue exclusion test. Results are mean ± SEM of 3 experiments. Significance of difference between control and absence of serum and between ± serum and absence of serum: $^*P < 0.001$ (Bonferroni multiple comparisons test). (For interpretation of the references to colour in this figure legend, the reader is referred to the web version of this article.)

blotting with anti-GAPDH or anti-ERK2 antibody (negative control) showed the co-precipitation of ERK5 with GAPDH only (Fig. 1B). GAPDH could also be co-immunoprecipitated with MEK5 (Fig. 1C) which binds ERK5 via the PB1 domain (discussed above). Similarly, ERK2 was not co-precipitated with MEK5 (Fig. 1C). Reverse immunoprecipitation and western blotting also show the co-immunoprecipitation of GAPDH and MEK5 (Fig. 1C, bottom panel). An equivalent amount of non-specific IgG did not precipitate the target proteins.

3.2. GAPDH binds directly to MEKK3

Given that the MEKK3-MEK5-ERK5 ternary complex also contains other proteins, including cerebral cavernous malformation 2 [28] and p62/sequestosome 1 [29], it was important to determine the identity of the protein/kinase that was responsible for binding GAPDH. As we have previously demonstrated that the anti-MEK5 antibody that we use disrupts the MEK5-ERK5 interaction [30], the data imply that GAPDH

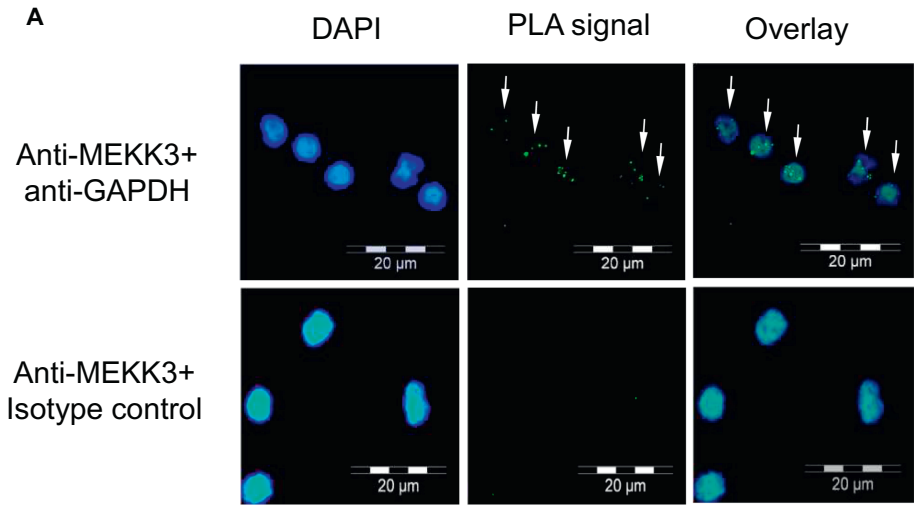

Fig. 4. GAPDH binds to MEKK3 in human peripheral blood T cells. T cells were prepared as described under Materials and Methods. They were cytocentrifuged onto glass slides and GAPDH-MEKK3 interaction analysed by the PLA assay. Arrows indicate the positions of PLA dots. Results are representative of 4 separate experiments.

did not bind directly to ERK5. Pull-down assays revealed that GST-MEK5 did not bind recombinant GAPDH (Fig. 2A). In contrast, we detected binding of HUVEC-derived GAPDH to GST-MEK5 (Fig. 2B). This implies that GAPDH did not bind directly to either MEK5 or ERK5 when it co-immunoprecipitated with these kinases (Fig. 1) but that another protein that was present in HUVEC was responsible for binding GAPDH, as well as binding GST-MEK5. We found that GST-MEKK3 pulled down recombinant GAPDH (Fig. 2C). These data establish that MEKK3 directly binds GAPDH.

3.3. Regulation of GAPDH-MEKK3 interaction in HUVEC by serum

Although the MEKK3-ERK5 module constitutes an important pathway for the survival-promoting actions of serum [5], its mechanism of action remains poorly understood. The above data suggest a cross-talk between MEKK3 and GAPDH in effecting their functions. We therefore investigated whether serum could regulate the interaction of GAPDH with MEKK3. A basal level of GAPDH-MEKK3 interaction was detected in HUVEC that had been cultured in the presence of serum for 4 days (Fig. 3A). Removal of serum (−) reduced such interaction to very low or undetectable levels. Replenishing the serum-depleted medium with fresh serum (±) not only re-established this interaction but it also caused a greater degree of GAPDH-MEKK3 binding than the basal level observed at 4 days of culture. This interaction could be observed in situ using the proximity ligation assay (PLA) (Fig. 3B). Cells were allowed to adhere to microscope cover glass overnight in the presence of 20% serum before being analysed. In control cells, PLA revealed GAPDH-MEKK3 interaction as discrete spots and these were visible in all cells, albeit in varying densities (Fig. 3B, top row). When the cells were washed and incubated in serum-free medium for 30 min (− serum, second row), the PLA spots were absent, indicating the absence of GAPDH-MEKK3 interaction. This interaction was re-established following the addition of fresh serum to the serum-starved cells (− serum, + serum)(third row). Under this serum-replenished condition, substituting the detecting antibodies with a control IgG gave little or no PLA signal (Fig. 3B, bottom row). The effects of serum depletion and replenishment on endothelial cell death and survival are shown in Fig. 3C. As expected, serum depletion reduced endothelial cell viability and this was prevented by adding fresh serum to serum-starved cells. These data demonstrate that viable cells contained GAPDH-MEKK3 complexes but these were lost during cell death induced by serum-deprivation. *Re*-addition of serum to serum-starved cells not only prevented cell death but it also re-established the MEKK3-GAPDH interaction.

3.4. GAPDH-MEKK3 interaction in human T cells

To ascertain whether the GAPDH-MEKK3 interaction was restricted to endothelial cells or not, we perform the PLA in human peripheral blood T cells. The data in Fig. 4 show that such interaction also occurred in human T cells (Fig. 4).

3.5. Serum depletion causes a disappearance of soluble MEKK3 and an increase in nuclear GAPDH

To gain an understanding of the basis for the loss of the GAPDH-MEKK3 interaction upon serum depletion, we investigated whether serum depletion would alter the levels of MEKK3 and GAPDH or affect their subcellular localisation in HUVEC. Interestingly, serum removal caused a rapid reduction in the level of cytosolic MEKK3 compared to control (Fig. 5A), detectable immediately post-wash (0 min) compared to control. MEKK3 was barely detectable by 5 and 20 min. Kinetic studies demonstrate that this loss of soluble MEKK3 was accompanied by a rapid loss of the MEKK3-GAPDH interaction (Fig. 5B). The level of nuclear MEKK3 was not affected by serum depletion (Fig. 5C).

In contrast, although serum depletion did not affect the level of cytoplasmic GAPDH, it caused an increase in the level of nuclear GAPDH (Fig. 5D). These data imply that the loss of soluble MEKK3 was a likely cause for the loss of MEKK3-GAPDH interaction and that a small proportion of GAPDH subsequently accumulated in the nucleus, without affecting the total level of cytoplasmic GAPDH.

3.6. Addition of serum to serum-starved cells restores soluble MEKK3 and nuclear GAPDH to pre-serum-depletion levels

The addition of fresh serum after 30 min of serum-depletion caused a rapid reappearance of MEKK3 in the cytosolic compartment (Fig. 5A). This argues against a degradation-resynthesis basis for the change in MEKK3 levels. As there was no detergent in the buffer used to prepare the cytosolic and nuclear fractions, one likely explanation is that MEKK3 had translocated to a particulate compartment in response to serum removal and relocated back into the cytoplasm upon serum replenishment. Kinetics studies show that the MEKK3-GAPDH interaction was rapidly re-established following the re-addition of serum to serum-starved cells (Fig. 5E) and that a minimum of 5% serum was necessary to re-establish this interaction (Fig. 5F). The degree of interaction increased with increasing serum concentration. Serum replenishment of serum-starved cells also caused a reduction in nuclear GADPH to a level that was similar to that in control cells (Fig. 5D).

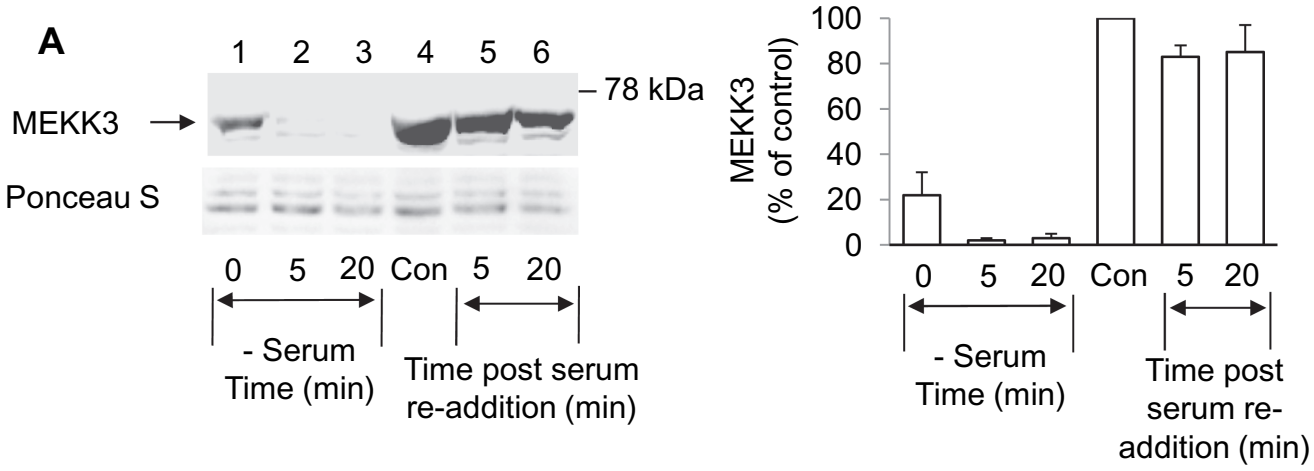

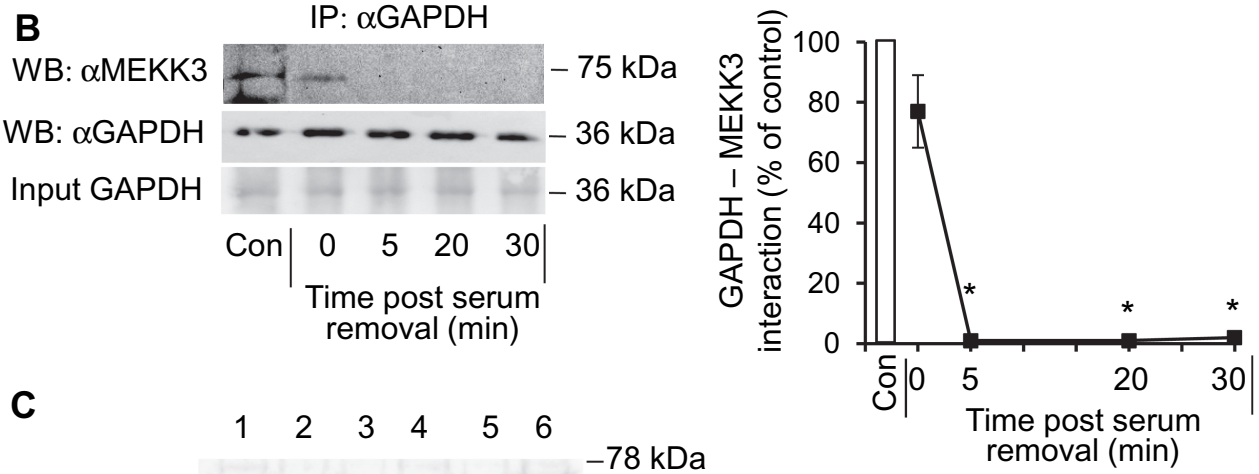

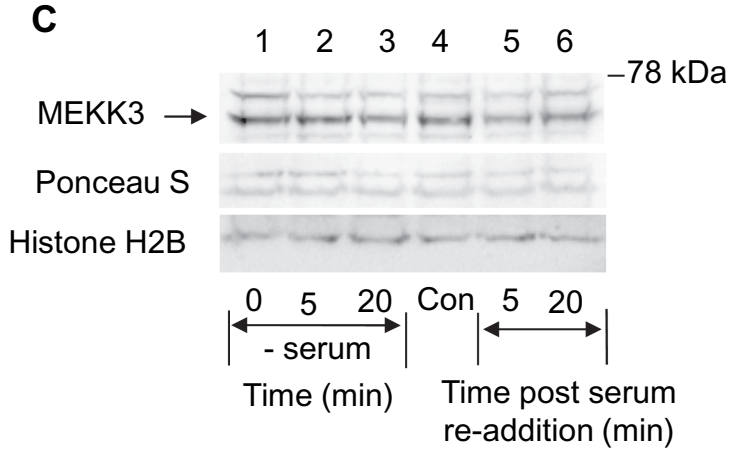

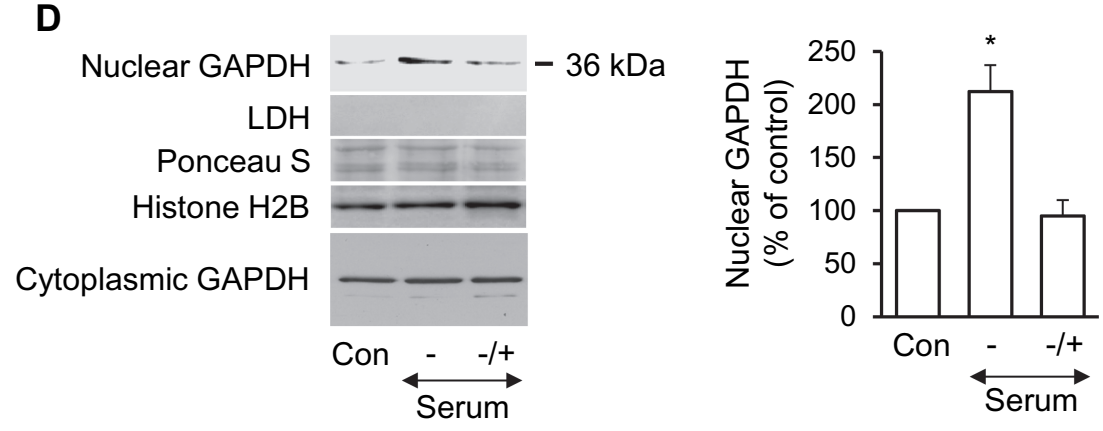

(caption on next page)

Fig. 5. Serum regulates the levels of soluble MEKK3 and nuclear GAPDH, in addition to the GAPDH-MEKK3 interaction. Panel (A, western blot and quantitated data) shows soluble MEKK3 and panel (C) shows nuclear MEKK3 from the same cells. HUVEC were either lysed (Con, lane 4) or washed in serum-free medium and incubated for the times indicated in the absence of serum (lanes 1–3). Another set of cells were washed with serum-free medium and incubated in this medium for 30 min (lane 5 and lane 6). The medium was then replenished with serum (20%) and the cells were incubated for either 5 or 20 min. The cells were lysed in detergent-free buffer to prepare cytosolic and nuclear fractions for the determination of MEKK3. Representative blots of 2 experiments and quantitated results (mean ± range, $n = 2$) are shown. (B) Rapid loss of GAPDH-MEKK3 binding upon removal of serum. One set of HUVEC were lysed at the start of the experiment (Con). The remaining cells were washed with serum-free medium and incubated in this medium for up to 30 min. The degree of GAPDH-MEKK3 binding was determined and quantitated. Significance of difference from control: $^{*}P < 0.001$ ($n = 3$ experiments)(Dunnett's test). (D) Serum depletion causes an increase in nuclear GAPDH. HUVEC were treated as follows: incubated in the original culture medium (Con), washed in serum-free medium and incubated in this medium for 5 h (−) or incubated in the absence of serum for 2 h and then in the presence of serum for 3 h (±). The cells were lysed and nuclear fractions were prepared for analysis of nuclear GAPDH. Quantitated data (histogram) are mean ± SEM of 5 separate experiments. Significance of difference between control and absence of serum and between absence of serum and ± serum: $^{*}P < 0.01$ (Bonferroni multiple comparisons test). (E) Time course of the re-establishment of GAPDH-MEKK3 interaction in response to serum. Following a 30 min incubation in the absence of serum, HUVEC were incubated with 20% serum for the indicated times, lysed and the degree of GAPDH-MEKK3 binding was determined. The results (mean ± SEM of 3 separate experiments) are expressed as % of control. Significance of difference between 0 min and higher time points: $^{*}P < 0.05$, $^{**}P < 0.01$, $^{***}P < 0.001$ (Dunnett's test). (F) Concentration-dependent effect of serum on the binding of GAPDH to MEKK3. One set of cells was lysed (Con) and the remaining were washed in serum-free medium and incubated in this medium for 30 min. The cells were then incubated with either buffer or 1–20% serum for 30 min, lysed and GAPDH-MEKK3 binding was determined. Results (mean ± SEM of 3 separate experiments) are expressed as % of control. Significance of difference from 0% serum: $^{*}P < 0.001$. Multiple comparisons were conducted using Dunnett's test.

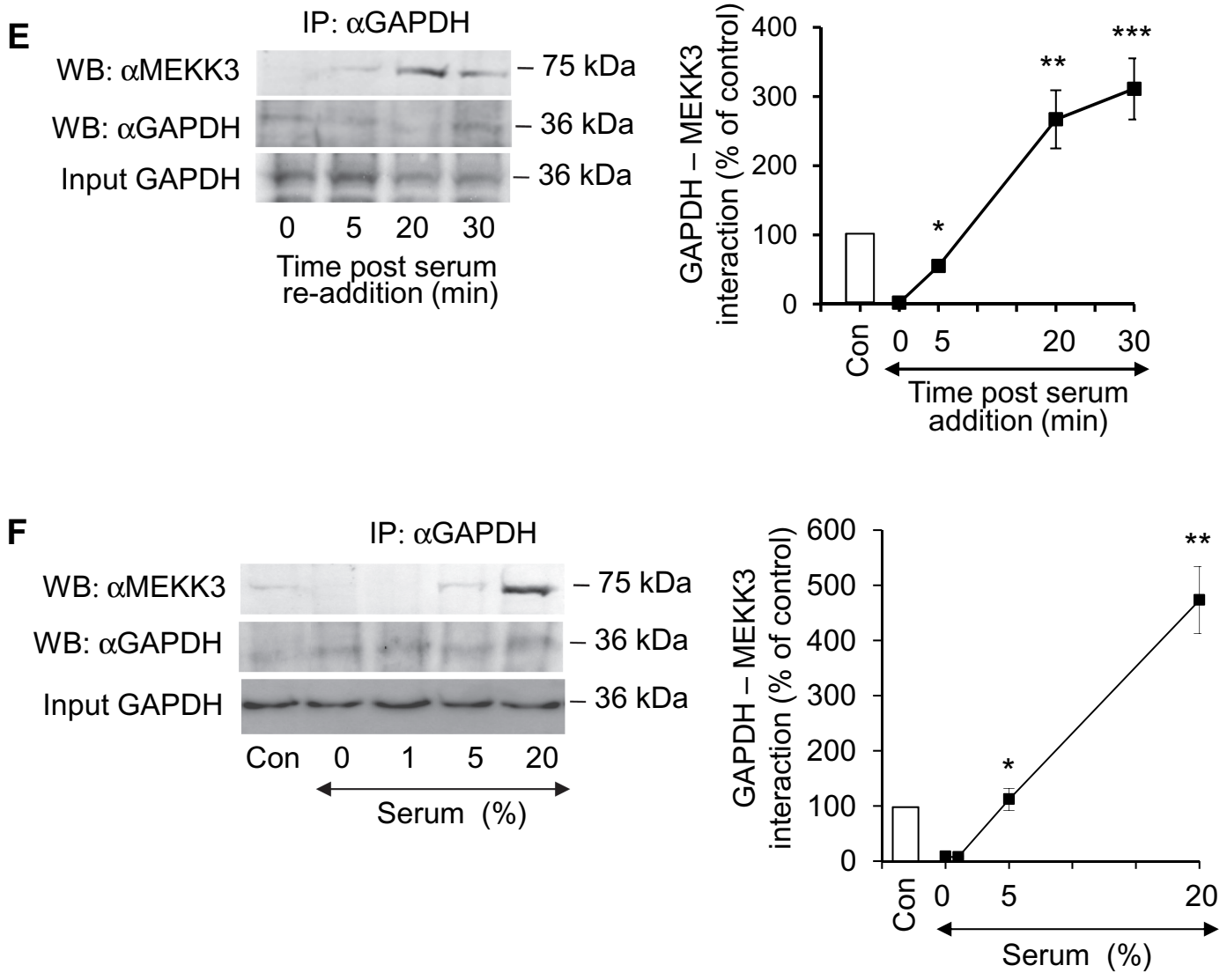

Fig. 5. (*continued*)

3.7. Cytotoxic concentrations of H_2O_2 cause an increase in nuclear GAPDH

To determine whether other inducers of endothelial cell death could also increase the level of nuclear GAPDH, we conducted similar studies using cytotoxic concentrations of H_2O_2. The data in Fig. 6A show that a cytotoxic concentration of H_2O_2 caused an increase in the level of nuclear GAPDH and this was accompanied by a reduction in cell viability (Fig. 6B). In contrast, a sub-cytotoxic concentration of 100 μM H_2O_2 did not affect either cell viability or the level of nuclear GAPDH (data not shown). Time course studies revealed that the effect of H_2O_2 on nuclear

GAPDH was time-dependent, reaching a statistically significant increase after 3 h (Fig. 6C).

3.8. Inhibition of nuclear accumulation of GAPDH reduces H_2O_2-mediated endothelial cell death

The above data suggest that an increase in nuclear GAPDH could trigger endothelial cell death, as had been reported in some cell-types [24,25]. The relationship between increases in nuclear GAPDH and cell viability was investigated using R-(−)-deprenyl hydrochloride, an agent that had previously been reported to inhibit apoptosis of neuronal cells owing to its ability to inhibit the nuclear translocation of GAPDH [24]. Initial dose-response studies revealed that R-(−)-deprenyl, at concentrations > 100 μM, reduced morphological signs of cell death following H_2O_2-treatment. The data in Fig. 7A show that pretreatment with R-(−)-deprenyl reduced the level of nuclear GAPDH in H_2O_2-treated cells and in those subjected to serum-starvation. When investigated in H_2O_2-treated cells, R-(−)-deprenyl-pretreatment reduced the cytotoxicity of H_2O_2 (Fig. 7B). Consequently, there were about 3 times more viable cells in the presence than in the absence of R-(−)-deprenyl following exposure to H_2O_2. These data are consistent with the concept that an increase in nuclear GAPDH acted as a trigger for endothelial cell death.

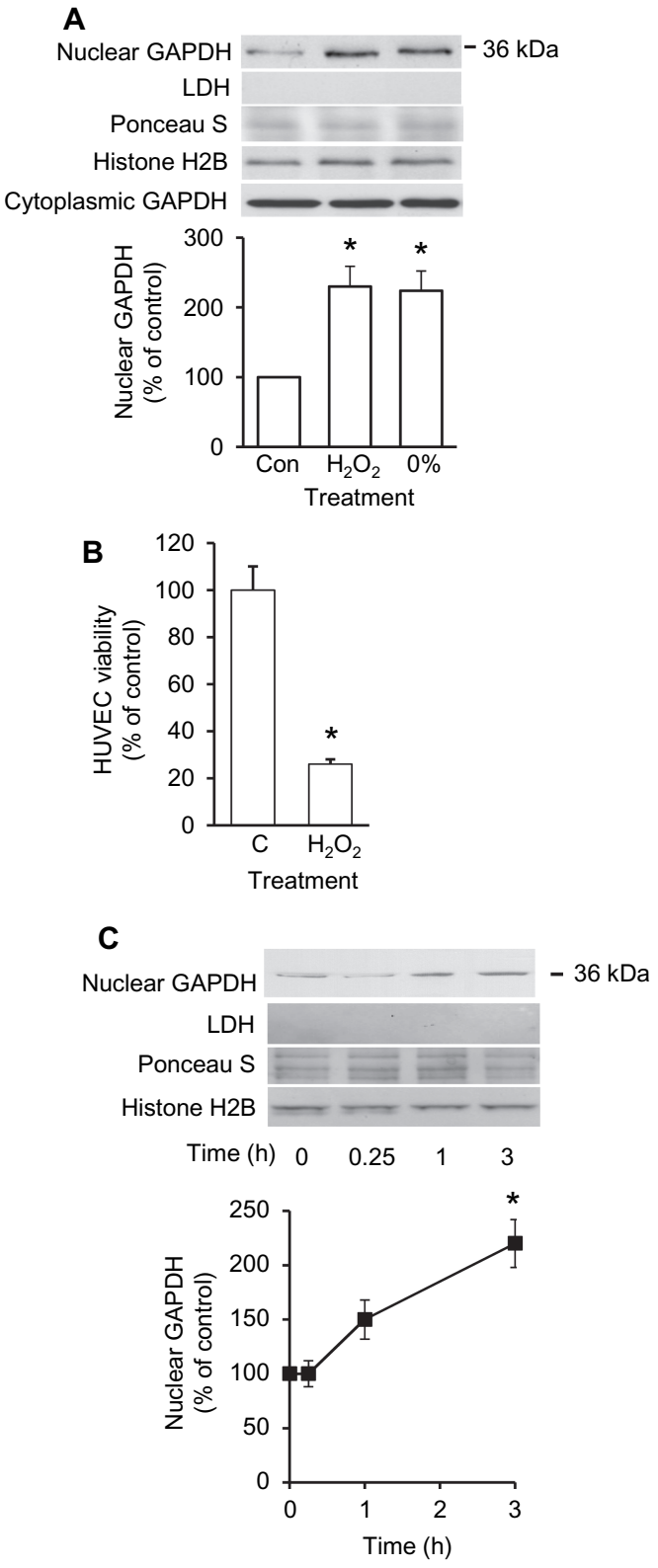

Fig. 6. Cytotoxic concentrations of H_2O_2 caused an increase in nuclear GAPDH and endothelial cell death. (A) HUVEC were incubated in the presence (Con) or absence of serum (0%), or with H_2O_2 (500 μM) for 5 h. Cytoplasmic and nuclear fractions were prepared for western blotting with anti-GAPDH antibody. Quantitated data are mean ± SEM of 4 separate experiments. Significance of difference versus control: $^*P < 0.05$ (Dunnett's test). (B) H_2O_2 reduces the viability of HUVEC. Cells were incubated with H_2O_2 for 15 h and cell viability was assessed by the trypan blue exclusion test. Results (mean ± SEM) are from 3 experiments. Significance of difference: $^*P < 0.001$ (Student's one-tailed *t*-test). (C) Time course of H_2O_2-stimulated increase in nuclear GAPDH. HUVEC were incubated with H_2O_2 for the times indicated and nuclear fractions were prepared to determine the levels of nuclear GAPDH. Quantitated data are mean ± SEM of at least 3 experiments. Significance of difference between 0 and 3 h: $^*P < 0.01$ (Dunnett's test).

3.9. Active MEKK3 phosphorylates GAPDH on 4 sites

In human cells cultured in the presence of serum, GAPDH is phosphorylated on a number of serine, threonine and tyrosine residues but none of the identified kinases are members of the MEKK3-ERK5 module [26,31,32]. The presence of a phosphorylated protein(s) with M_r of ~36,000 in Fig. 1A prompted us to investigate whether GAPDH could be phosphorylated by MEKK3. A cell-free kinase assay using recombinant proteins in the presence of ^{32}P-ATP was employed to investigate this possibility. Whereas an inactive, bacteria-expressed GST-MEKK3 did not phosphorylate recombinant GAPDH despite its ability to bind GAPDH (Fig. 2C), active GST-MEKK3 (expressed in Sf9 insect cells) phosphorylated GAPDH in an incubation time-dependent manner (Fig. 8). A fresh non-radioactive sample of MEKK3-phosphorylated GAPDH was then subjected to SDS PAGE and the GAPDH band excised and was digested with either trypsin or ASP-N. The peptides were applied to LC-eSI-MS/MS in a LTQ Orbitrap XL™ Hybrid Ion Trap-Orbitrap mass spectrometer. Three regions in GAPDH were found to contain phosphorylation sites (Table 2).

The mass of each peptide corresponded to a single phosphorylation. While we were able to unambiguously identify S192 (Region 1, Table 2) as a phosphorylation site, the presence of 2 or more potential sites, for example S210 and T211 in one of the other peptides (Region 2, Table 2), made it difficult to unambiguously assign the site of phosphorylation (see Fig. 9 for CID spectra for the peptide containing S192 and the other containing S210 and T211). Nevertheless, on the basis that there was only one phosphosite/peptide, we deduced that S292 as another phosphosite in region 3.

4. Discussion

A search for novel collaborators of the MEKK3-ERK5 module as a means to further elucidate the mechanism of action of the kinase module in endothelial cells led to the discovery of a number of proteins

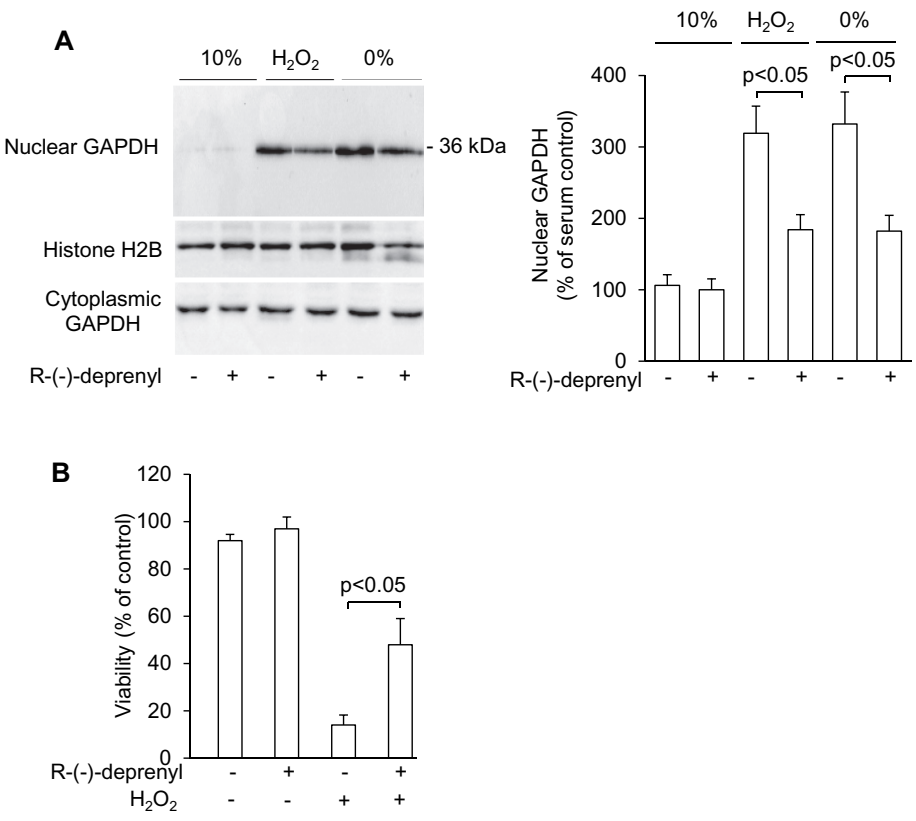

Fig. 7. R-(−)-deprenyl-pretreatment attenuated H_2O_2-stimulated nuclear accumulation of GAPDH and cell death. (A) HUVEC were preincubated with vehicle (DMSO) (0.01%, *v*/v) or R-(−)-deprenyl (100 μM) for 1 h before being treated with H_2O_2 (500 μM) or subjected to serum deprivation (0%). Control cells, in medium containing 10% serum, received buffer. Nuclear fractions were prepared after 4.5 h and were western blotted with anti-GAPDH antibody. A representative blot and quantitated data (mean ± SEM from 3 experiments with different batches of cells) are shown. (B) HUVEC were preincubated with R-(−)-deprenyl or vehicle for 1 h, followed by the addition of H_2O_2. The cells were incubated for 16 h and viability was determined. Results are mean ± SEM of 3 experiments with different batches of cells. Statistical analyses were conducted using Student's one-tailed *t*-test.

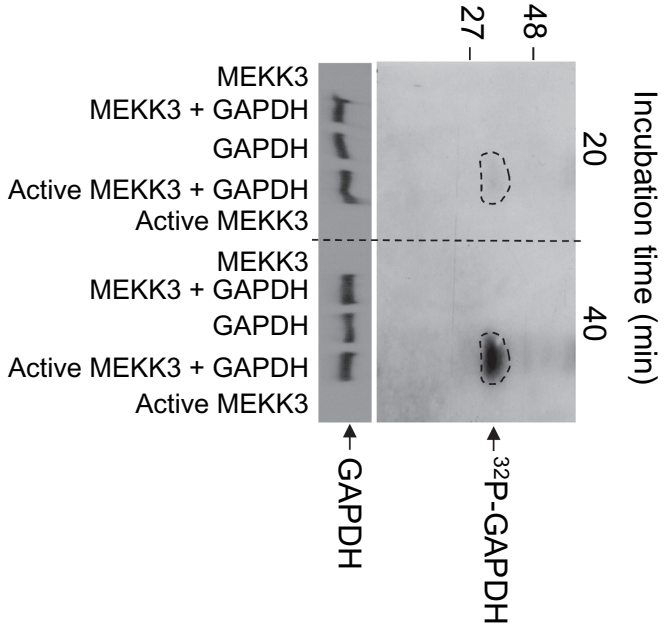

Fig. 8. Phosphorylation of GAPDH by active MEKK3. (A) Recombinant GAPDH (1 μg) was incubated with either inactive GST-MEKK3 or active GST-MEKK3 (0.2 μg each) in assay buffer containing ^{32}P-ATP for either 20 or 40 min at room temperature. The proteins were fractionated by SDS PAGE followed by autoradiography or western blotting with anti-GAPDH antibody to detect GAPDH. A representative autoradiogram (top) and western blot (bottom) of 3 experiments, all with similar results, are shown.

that co-immunoprecipitated with ERK5, implicating the existence of an interactome. Querying the GO-Biological process enabled these proteins to be placed in functional groups that cover energy metabolism, mitochondrial function, cell survival and death, ribosomal function, protein synthesis and folding, and chaperones. This implies that the MEKK3-ERK5 module may play a role in regulating these processes but this remains to be determined. Focusing on the regulation of cell death and guided by factors such as molecular weight, phosphorylation status and ability to cause cell death, we selected GAPDH for characterisation and confirmed it as a novel component of the MEKK3-ERK5 ternary complex, through a direct binding to MEKK3. This MEKK3-GAPDH interaction was also detected in human T cells, demonstrating that this relationship is not restricted to endothelial cells.

The GAPDH-kinase interaction was not static. Under conditions that favoured cell survival e.g. culturing the cells in the presence of serum, there was a basal level of both the GAPDH-MEKK3 interaction and nuclear GAPDH. Upon serum deprivation, a trigger for endothelial cell death, there was a rapid loss of both soluble MEKK3 and the GAPDH-MEKK3 interaction. This was accompanied by an increase in the level of nuclear GAPDH. Given that the disappearance of soluble MEKK3 and the loss of the GAPDH-MEKK3 interaction occurred with similar kinetics, we postulate that the disappearance of MEKK3 liberated GAPDH from the kinase complex, thereby explaining the loss of GAPDH-MEKK3 interaction. Whether this then enabled the accumulation of GAPDH in the nucleus remains to be determined. However, it has previously been reported that serum stimulates the efflux of GAPDH from the nucleus [27]. Consequently, in the absence of serum, there would be less efflux of GAPDH from the nucleus, contributing to an increase in nuclear GAPDH.

Addition of fresh serum to serum-starved cells reversed the changes caused by serum-deprivation and prevented cell death. Since the effect of serum on the reappearance of MEKK3 was rapid and there was no increase in MEKK3 in the nucleus, the data support the likelihood that MEKK3 had moved to an insoluble fraction in the absence of serum, rather than being degraded. This would account for the rapid reappearance of soluble MEKK3 upon serum replenishment. The reduction in nuclear GAPDH upon serum-replenishment was likely achieved by a serum-stimulated efflux of GAPDH from the nucleus [27], as discussed above. The net effect of these is the re-establishment of the

Table 2
Identification of MEKK3 phospho-targets in GAPDH.

	Protease	Residues	Peptide[a,b]
Region 1	Trypsin	163–186	K.VIHDNFGIVEGLMTTVHAITATQK.T
	Asp-N	166–188	H.DNFGIVEGLMTTVHAITATQKTV.D
	Trypsin	187–197	K.TVDGPSGKLWR.D
Region 2	Trypsin	201–215	R.GALQNIIPASTGAAK.A
Region 3	Trypsin	272–309	K.GILGYTEHQVVSSDFNSDTHSSTFDAGAGIALNDHFVK.L
	Asp-N	285–295	S.DFNSDTHSSTF.D
	Asp-N	289–304	S.DTHSSTFDAGAGIALN.D

[a] In each instance, the mass of the detected peptide corresponds to a single phosphorylation.
[b] Where more than one site is underlined, it is not possible from the data to unambiguously assign the site of phosphorylation (due to the complexity of the fragmentation, and the number and grouping of possible sites). S192 is a phosphosite and by deduction, S292 is a phosphosite. It is not possible to distinguish phosphorylation between T176 and T177, and between S210 and T211.

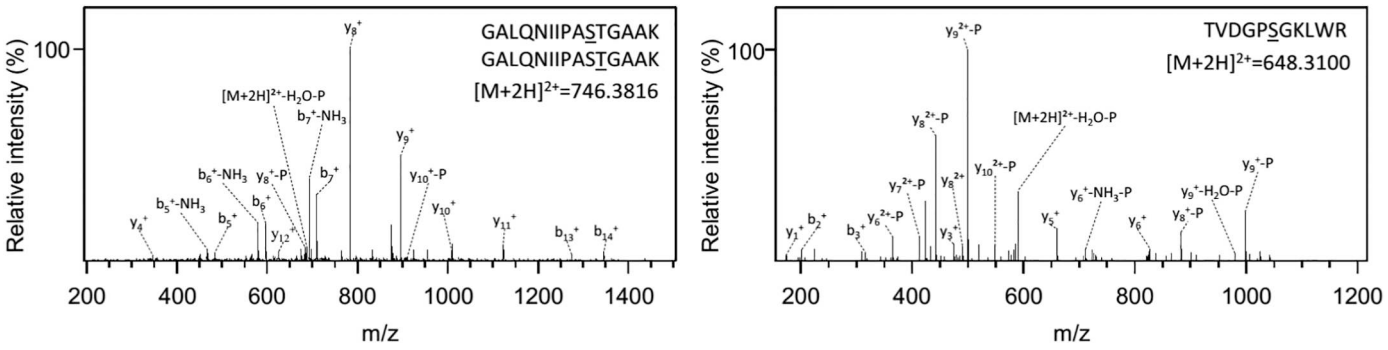

Fig. 9. Collision induced dissociation (CID) spectra of GADPH-derived peptides G_{201}ALQNIIPASTGAAK$_{215}$ and T_{187}VDGPSGKLWR$_{197}$, 746.3816 *m/z* and 648.3100 *m/z*, respectively. From the observed fragments of G_{201}ALQNIIPASTGAAK$_{215}$ it was not possible to discriminate between phosphorylation of S_{210} or T_{211}. Phosphorylation of S_{192} of T_{187}VDGPSGKLWR$_{197}$ was confirmed by the observed fragment ions.

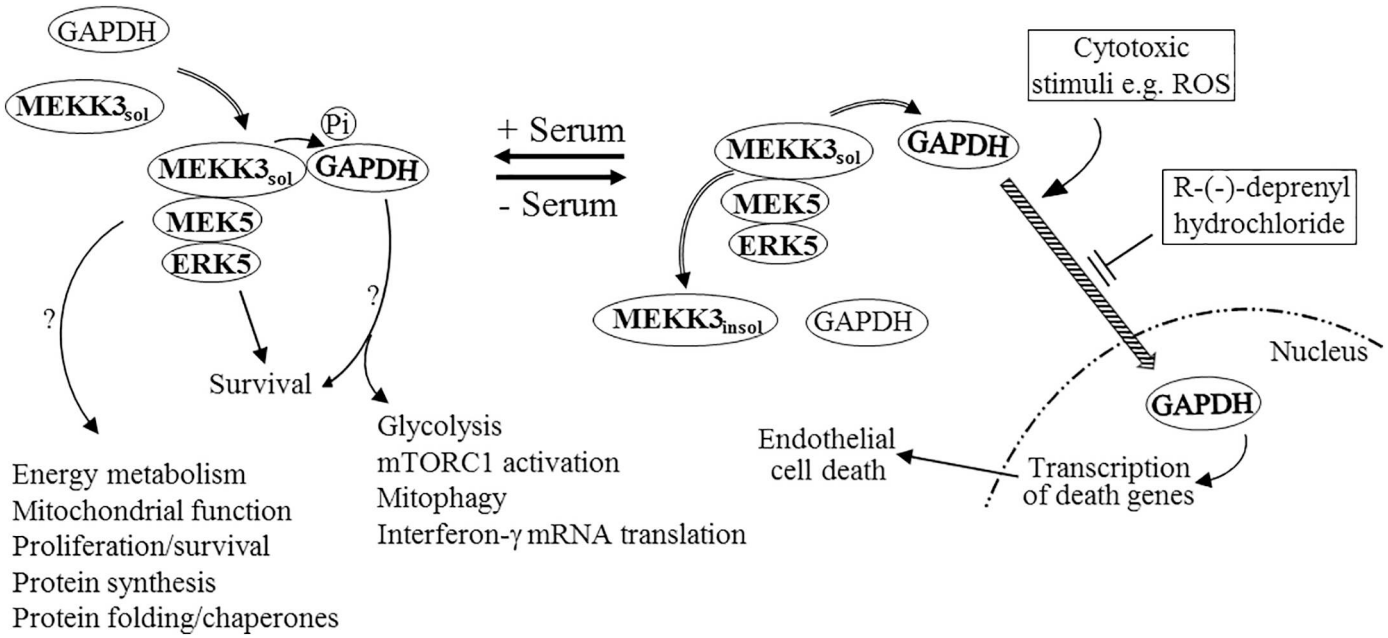

Fig. 10. A model depicting new modes of action of the MEKK3-ERK5 module in endothelial cells and nuclear GAPDH as a trigger of endothelial cell death. The MEKK3-ERK5 module regulates not only endothelial cell survival but also potentially other cellular processes. Cell survival is associated with MEKK3-GAPDH interaction. Cell death is associated with the loss of this interaction and is triggered by an increase in nuclear GAPDH. Phosphorylation of GAPDH by MEKK3 provides MEKK3 with an avenue to regulate GAPDH function. Double-lined arrows: promotion or loss of protein-protein interaction. Striped arrow: nuclear translocation. Question marks indicate potential roles that remain to be determined.

MEKK3-GAPDH interaction.

The data are consistent with the concept that an increase in nuclear GAPDH acted as a trigger for endothelial cell death. Consistent with this, we have found that cytotoxic concentrations of H_2O_2 increased the level of nuclear GAPDH, as had been reported in a neuroblastoma cell line [33], whereas sub-cytotoxic concentrations of H_2O_2 did not. A cytotoxic combination of tumour necrosis factor α and cycloheximide also increased the level of nuclear GAPDH in HUVEC (not shown). As

discussed, addition of fresh serum to serum-starved cells not only caused a reduction in the level of nuclear GAPDH but also prevented cell death. More importantly, treatment of the cells with R-(−)-deprenyl, a known inhibitor of the nuclear translocation of GAPDH that also protected against GAPDH-mediated death of RAW264.7 cells and neurones [24], led to a reduction of H_2O_2-mediated cytotoxicity. Although R-(−)-deprenyl, prescribed for patients with Parkinson's disease, is a known inhibitor of monoamine oxidase-B, its protective action against cell death and its mode of action as a neuro-protector were independent of monoamine oxidase [25]. These observations strongly support the notion that nuclear GAPDH is a trigger of endothelial cell death.

Another novel finding is that GAPDH is a substrate for MEKK3. The cell free assays have identified S192 as an MEKK3 phosphosite and, by deduction, we have assigned S292 as another MEKK3 phosphosite. NetPhos 3.1 (score > 0.5) predicts unspecified kinases phosphorylating both S192 and S292, raising the possibility that MEKK3 is one such kinase. Two other sites, either T177 or T182 and either S210 or T211, were also phosphorylated by recombinant MEKK3. However, T177 and T182 are predicted sites (NetPhos 3.1) for protein kinase C and casein kinase 1, respectively, and S210 and T211 are predicted sites for protein kinase C. Interestingly, phosphorylation of these amino acid residues has been detected previously in cells even though the responsible kinase(s) has(have) not been identified. Thus, T211 and S210 in GAPDH are phosphorylated in HeLa cells in G1 phase whilst T182 is phosphorylated in M phase [26]. In mouse liver, T177 and T182 have been found to be phosphorylated [34]. In HEK293T cells, Seo et al. [35] reported that T176 and T177 became phosphorylated in response to H_2O_2. In colorectal cancer tissues and cell lines, S192 and S210 are phosphorylated [36]. Whether MEKK3 is one of the kinases that target these sites remains to be investigated. Nevertheless, it is likely that the phosphorylation of GAPDH by MEKK3 would enable direct regulation of the function of GAPDH as a mediator of cell death and in its other roles, including glycolysis, mTORC1 activation [37], interferon γ mRNA translation in T cells [38] and mitophagy-associated protection from caspase-independent cell death [39].

5. Conclusions

In summary, the data support a role for an increase in nuclear GAPDH in causing endothelial cell death in response to serum-deprivation and cytotoxic concentrations of H_2O_2. The data also reveal an avenue for direct cross-talking between the pro-survival MEKK3 and GAPDH, through the binding and phosphorylation of GAPDH by MEKK3. We propose that GAPDH phosphorylation by MEKK3 represents a novel mechanism through which the kinase blocks the death-inducing role of GAPDH and promotes endothelial cell survival, independently of the downstream MEK5 and ERK5. The data from the co-immunoprecipitation studies, although awaiting validation, suggest possible roles of the MEKK3-ERK5 module in regulating functions such as energy metabolism, protein synthesis and folding, and chaperones, in addition to regulating endothelial cell death and survival (Fig. 10).

Funding information

This work was supported by grants from the National Heart Foundation of Australia (G06A 2483, G08A-3654), National Health and Medical Research Council of Australia, and the Women's and Children's Hospital Research Foundation. The funding sources had no influence or involvement in the investigations or the preparation of the manuscript.

Conflict of interest

The authors declare that they have no conflicts of interest.

Author contribution

Y.Q.L. conducted most of the experiments and participated in data analysis. AN performed the PLA studies. The proteomics work was conducted in the laboratory of P.H., under P.H.'s supervision. C.H. conceived the idea for the project, planned the experiments, conducted some of the cell survival studies, analysed the data and wrote the manuscript with input from P.H. and A.F. All authors have approved the final article.

Declarations of interest

None.

References

[1] R. Ross, Atherosclerosis—an inflammatory disease, N. Engl. J. Med. 340 (1999) 115–126, https://doi.org/10.1056/NEJM199901143400207.
[2] P.R. Coleman, C.N. Hahn, M. Grimshaw, Y. Lu, X. Li, P.J. Brautigan, K. Beck, R. Stocker, M.A. Vadas, J.R. Gamble, Stress-induced premature senescence mediated by a novel gene, SENEX, results in an anti-inflammatory phenotype in endothelial cells, Blood 116 (2010) 4016–4024, https://doi.org/10.1182/blood-2009-11-252700.
[3] J.S. Pober, W. Min, J.R. Bradley, Mechanisms of endothelial dysfunction, injury, and death, Annu. Rev. Pathol. 4 (2009) 71–95, https://doi.org/10.1146/annurev.pathol.4.110807.092155.
[4] I. Tabas, G. García-Cardeña, G.K. Owens, Recent insights into the cellular biology of atherosclerosis, J. Cell Biol. 209 (2015) 13–22, https://doi.org/10.1083/jcb.201412052.
[5] X. Pi, C. Yan, B.C. Berk, BMK1/ERK5 protects endothelial cells from apoptosis, Circ. Res. 94 (2004) 362–369, https://doi.org/10.1161/01.RES.0000112406.27800.6F.
[6] M.G. Scioli, A. Bielli, S. Agostinelli, C. Tarquini, G. Arcuri, A. Ferlosio, G. Costanza, E. Doldo, A. Orlandi, Antioxidant treatment prevents serum deprivation- and TNF-α-induced endothelial dysfunction through the inhibition of NADPH oxidase 4 and the restoration of β-oxidation, J. Vasc. Res. 51 (2014) 327–337, https://doi.org/10.1159/000365926.
[7] G.N. Nithianandarajah-Jones, B. Wilm, C.E. Goldring, J. Müller, M.J. Cross, The role of ERK5 in endothelial cell function, Biochem. Soc. Trans. 42 (2014) 1584–1589, https://doi.org/10.1042/BST20140276.
[8] J. Yang, M. Boerm, M. McCarty, C. Bucana, I.J. Fidler, Y. Zhuang, B. Su, Mekk3 is essential for early embryonic cardiovascular development, Nat. Genet. 24 (2000) 309–313, https://doi.org/10.1038/73550.
[9] X. Wang, A.J. Merritt, J. Seyfried, C. Guo, E.S. Papadakis, K.G. Finegan, M. Kayahara, J. Dixon, R.P. Boot-Handford, E.J. Cartwright, U. Mayer, C. Tournier, Targeted deletion of MEK5 causes early embryonic death and defects in the ERK5/MEF2 cell survival pathway, Mol. Cell. Biol. 25 (2005) 336–345, https://doi.org/10.1128/MCB.25.1.336-345.2005.
[10] C.P. Regan, W. Li, D.M. Boucher, S. Spatz, M.S. Su, K. Kuida, Erk5 null mice display multiple extraembryonic vascular and embryonic cardiovascular defects, Proc. Natl. Acad. Sci. U. S. A. 99 (2002) 9248–9253, https://doi.org/10.1073/pnas.142293999.
[11] Y. Deng, J. Yang, M. McCarty, B. Su, MEKK3 is required for endothelium function but is not essential for tumor growth and angiogenesis, Am. J. Phys. Cell Physiol. 293 (2007) C1404–C1411, https://doi.org/10.1152/ajpcell.00058.2007.
[12] M. Hayashi, S.W. Kim, K. Imanaka-Yoshida, T. Yoshida, E.D. Abel, B. Eliceiri, Y. Yang, R.J. Ulevitch, J.D. Lee, Targeted deletion of BMK1/ERK5 in adult mice perturbs vascular integrity and leads to endothelial failure, J. Clin. Invest. 113 (2004) 1138–1148, https://doi.org/10.1172/JCI19890.
[13] Z.H. Huang, E.J. Bates, J.V. Ferrante, C.S. Hii, A. Poulos, B.S. Robinson, A. Ferrante, Inhibition of stimulus-induced endothelial cell intercellular adhesion molecule-1, E-selectin, and vascular cellular adhesion molecule-1 expression by arachidonic acid and its hydroxy and hydroperoxy derivatives, Circ. Res. 80 (1997) 149–158 (PMID: 9012737).
[14] H.P. Jersmann, C.S. Hii, G.L. Hodge, A. Ferrante, Synthesis and surface expression of CD14 by human endothelial cells, Infect. Immun. 69 (2001) 479–485, https://doi.org/10.1128/IAI.69.1.479-485.2001.
[15] C.S. Hii, M. Costabile, G.C. Mayne, C.J. Der, A.W. Murray, A. Ferrante, Selective deficiency in protein kinase C isoenzyme expression and inadequacy in mitogen-activated protein kinase activation in cord blood T cells, Biochem. J. 370 (2003) 497–503, https://doi.org/10.1042/BJ20021122.
[16] C.S. Hii, Z.H. Huang, A. Bilney, M. Costabile, A.W. Murray, D.A. Rathjen, C.J. Der, A. Ferrante, Stimulation of p38 phosphorylation and activity by arachidonic acid in HeLa cells, HL60 promyelocytic leukemic cells, and human neutrophils. Evidence for cell type-specific activation of mitogen-activated protein kinases, J. Biol. Chem. 273 (1998) 19277–19282 (PMID: 9668117).
[17] N.C. Andrews, D.V. Faller, A rapid micropreparation technique for extraction of DNA-binding proteins from limiting numbers of mammalian cells, Nucleic Acids Res. 19 (1991) 2499 (PMID: 2041787).
[18] K. Nakamura, M.T. Uhlik, N.L. Johnson, K.M. Hahn, G.L. Johnson, PB1 domain-dependent signaling complex is required for extracellular signal-regulated kinase 5 activation, Mol. Cell. Biol. 26 (2006) 2065–2079, https://doi.org/10.1128/MCB.

26.6.2065-2079.2006.
[19] K. Nakamura, G.L. Johnson, Noncanonical function of MEKK2 and MEK5 PB1 domains for coordinated extracellular signal-regulated kinase 5 and c-Jun N-terminal kinase signaling, Mol. Cell. Biol. 27 (2007) 4566–4577, https://doi.org/10.1128/MCB.00125-07.
[20] C.H. Woo, T. Shishido, C. McClain, J.H. Lim, J.D. Li, J. Yang, C. Yan, J. Abe, Extracellular signal-regulated kinase 5 SUMOylation antagonizes shear stress-induced anti-inflammatory response and endothelial nitric oxide synthase expression in endothelial cells, Circ. Res. 102 (2008) 538–545, https://doi.org/10.1161/CIRCRESAHA.107.156877.
[21] J.M. English, C.A. Vanderbilt, S. Xu, S. Marcus, M.H. Cobb, Isolation of MEK5 and differential expression of alternatively spliced forms, J. Biol. Chem. 270 (1995) 28897–28902 7499418.
[22] J.M. English, G. Pearson, R. Baer, M.H. Cobb, Identification of substrates and regulators of the mitogen-activated protein kinase ERK5 using chimeric protein kinases, J. Biol. Chem. 273 (1998) 3854–3860.
[23] C.J. Valvona, H.L. Fillmore, P.B. Nunn, G.J. Pilkington, The regulation and function of lactate dehydrogenase A: therapeutic potential in brain tumor, Brain Pathol. 26 (2016) 3–17, https://doi.org/10.1111/bpa.12299.
[24] M.R. Hara, B. Thomas, M.B. Cascio, B.I. Bae, L.D. Hester, V.L. Dawson, T.M. Dawson, A. Sawa, S.H. Snyder, Neuroprotection by pharmacologic blockade of the GAPDH death cascade, Proc. Natl. Acad. Sci. U. S. A. 103 (2006) 3887–3889, https://doi.org/10.1073/pnas.0511321103.
[25] W. Tatton, R. Chalmers-Redman, N. Tatton, Neuroprotection by deprenyl and other propargylamines: glyceraldehyde-3-phosphatedehydrogenase rather than monoamine oxidase B, J. Neural Transm. (Vienna) 110 (2003) 509–515, https://doi.org/10.1007/s00702-002-0827-z.
[26] N. Dephoure, C. Zhou, J. Villén, S.A. Beausoleil, C.E. Bakalarski, S.J. Elledge, S.P. Gygi, A quantitative atlas of mitotic phosphorylation, Proc. Natl. Acad. Sci. U. S. A. 105 (2002) 10762–10767, https://doi.org/10.1073/pnas.0805139105.
[27] H.J. Kwon, J.H. Rhim, I.S. Jang, G.E. Kim, S.C. Park, E.J. Yeo, Activation of AMP-activated protein kinase stimulates the nuclear localization of glyceraldehyde 3-phosphatedehydrogenase in human diploid fibroblasts, Exp. Mol. Med. 42 (2010) 254–269, https://doi.org/10.3858/emm.2010.42.4.025.
[28] X. Cullere, E. Plovie, P.M. Bennett, C.A. MacRae, T.N. Mayadas, The cerebral cavernous malformation proteins CCM2L and CCM2 prevent the activation of the MAP kinase MEKK3, Proc. Natl. Acad. Sci. U. S. A. 112 (2015) 14284–14289, https://doi.org/10.1073/pnas.1510495112.
[29] K. Nakamura, A.J. Kimple, D.P. Siderovski, G.L. Johnson, PB1 domain interaction of p62/sequestosome 1 and MEKK3 regulates NF-kappaB activation, J. Biol. Chem. 285 (2010) 2077–2089, https://doi.org/10.1074/jbc.M109.065102.
[30] C.S. Hii, D.S. Anson, M. Costabile, V. Mukaro, K. Dunning, A. Ferrante, Characterisation of the MEK5-ERK5 module in human neutrophils and its relationship to ERK1/ERK2 in the chemotactic response, J. Biol. Chem. 279 (2004) 49825–49834, https://doi.org/10.1074/jbc.M406892200.
[31] E.J. Tisdale, Glyceraldehyde-3-phosphate dehydrogenase is phosphorylated by protein kinase Ciota/lambda and plays a role in microtubule dynamics in the early secretory pathway, J. Biol. Chem. 277 (2002) 3334–3341, https://doi.org/10.1074/jbc.M109744200.
[32] G. Yogalingam, S. Hwang, J.C. Ferreira, D. Mochly-Rosen, Glyceraldehyde-3-phosphate dehydrogenase (GAPDH) phosphorylation by protein kinase Cδ (PKCδ) inhibits mitochondria elimination by lysosomal-like structures following ischemia and reoxygenation-induced injury, J. Biol. Chem. 288 (2013) 18947–18960, https://doi.org/10.1074/jbc.M113.466870.
[33] Z. Dastoor, J.L. Dreyer, Potential role of nuclear translocation of glyceraldehyde-3-phosphate dehydrogenase in apoptosis and oxidative stress, J. Cell Sci. 114 (2001) 1643–1653 (PMID: 11309196).
[34] Y. Bian, C. Song, K. Cheng, M. Dong, F. Wang, J. Huang, D. Sun, L. Wang, M. Ye, H. Zou, An enzyme assisted RP-RPLC approach for in-depth analysis of human liver phosphoproteome, J. Proteome 96 (2014) 253–262, https://doi.org/10.1016/j.jprot.2013.11.014.
[35] J. Seo, J. Jeong, Y.M. Kim, N. Hwang, E. Paek, K.J. Lee, Strategy for comprehensive identification of post-translational modifications in cellular proteins, including low abundant modifications: application to glyceraldehyde-3-phosphate dehydrogenase, J. Proteome Res. 7 (2008) 587–602, https://doi.org/10.1021/pr700657y.
[36] T. Shiromizu, J. Adachi, S. Watanabe, T. Murakami, T. Kuga, S. Muraoka, T. Tomonaga, Identification of missing proteins in the neXtProt database and unregistered phosphopeptides in the PhosphoSitePlus database as part of the chromosome-centric human proteome project, J. Proteome Res. 12 (2013) 2414–2421, https://doi.org/10.1021/pr300825v.
[37] M.N. Lee, S.H. Ha, J. Kim, A. Koh, C.S. Lee, J.H. Kim, H. Jeon, D.H. Kim, P.G. Suh, S.H. Ryu, Glycolytic flux signals to mTOR through GAPDH-mediated regulation of Rheb, Mol. Cell. Biol. 29 (2009) 3991–4001, https://doi.org/10.1128/MCB.00165-09.
[38] C.H. Chang, J.D. Curtis, L.B. Maggi Jr., B. Faubert, A.V. Villarino, D. O'Sullivan, S.C. Huang, G.J. van der Windt, J. Blagih, J. Qiu, J.D. Weber, E.J. Pearce, R.G. Jones, E.L. Pearce, Posttranscriptional control of T cell effector function by aerobic glycolysis, Cell 153 (2013) 1239–1251, https://doi.org/10.1016/j.cell.2013.05.016.
[39] A. Colell, J.E. Ricci, S. Tait, S. Milasta, U. Maurer, L. Bouchier-Hayes, P. Fitzgerald, A. Guio-Carrion, N.J. Waterhouse, C.W. Li, B. Mari, P. Barbry, D.D. Newmeyer, H.M. Beere, D.R. Green, GAPDH and autophagy preserve survival after apoptotic cytochrome c release in the absence of caspase activation, Cell 129 (2007) 983–997, https://doi.org/10.1016/j.cell.2007.03.045.